Nuclear Import of *Arabidopsis* Poly(ADP-Ribose) Polymerase 2 Is Mediated by Importin-α and a Nuclear Localization Sequence Located Between the Predicted SAP Domains

Chao Chen, Raffaella De Masi, Ruth Lintermann and Lennart Wirthmueller*

Department of Plant Biochemistry, Dahlem Centre of Plant Sciences, Institute of Biology, Freie Universität Berlin, Berlin, Germany

Proteins of the Poly(ADP-Ribose) Polymerase (PARP) family modify target proteins by covalent attachment of ADP-ribose moieties onto amino acid side chains. In *Arabidopsis*, PARP proteins contribute to repair of DNA lesions and modulate plant responses to various abiotic and biotic stressors. *Arabidopsis* PARP1 and PARP2 are nuclear proteins and given that their molecular weights exceed the diffusion limit of nuclear pore complexes, an active import mechanism into the nucleus is likely. Here we use confocal microscopy of fluorescent protein-tagged *Arabidopsis* PARP2 and PARP2 deletion constructs in combination with site-directed mutagenesis to identify a nuclear localization sequence in PARP2 that is required for nuclear import. We report that in co-immunoprecipitation assays PARP2 interacts with several isoforms of the importin-α group of nuclear transport adapters and that PARP2 binding to IMPORTIN-α2 is mediated by the identified nuclear localization sequence. Our results demonstrate that PARP2 is a cargo protein of the canonical importin-α/β nuclear import pathway.

Keywords: Poly(ADP-Ribose) Polymerase, PARP2, nuclear localization sequence, nucleo-cytoplasmic transport, importin-α, *Arabidopsis thaliana*

INTRODUCTION

The post-translational modification of proteins is an important component of plant responses to changes in their environment. Post-translational modifications (PTMs) are often rapid and reversible processes that allow plants to fine-tune the speed and duration of stress-induced signaling. Numerous PTMs have been described in plants including phosphorylation, ubiquitination, SUMOylation, acetylation, and methylation (Hashiguchi and Komatsu, 2017; Withers and Dong, 2017). The N-terminal regions of the core histones are considered PTM hot spots and modification of histone tails plays a crucial role in transcriptional regulation and epigenetic processes including plant stress memory (Kleinmanns and Schubert, 2014; Asensi-Fabado et al., 2017).

Protein ADP-ribosylation is a PTM that recently has gained increasing attention in plants (Jia et al., 2013; Song et al., 2015; Feng et al., 2016; Vainonen et al., 2016; Rissel et al., 2017). Enzymes of the ADP-ribosyl transferase family catalyze covalent modification of proteins

and DNA with ADP-ribose. In mammalian cells, ADP-ribosyl transferases play important roles in several cellular pathways including, amongst others, DNA damage repair, apoptosis, transcriptional regulation, mRNA stability, and the cell cycle (Bai, 2015; Bock et al., 2015). Some ADP-ribosyl transferases catalyze the formation of poly-ADP-ribose chains by using the terminal ADP-ribose transferred onto an acceptor molecule as a substrate for subsequent rounds of ADP-ribosylation. These ADP-ribosyl transferases are also called Poly(ADP-Ribose) Polymerase (PARPs). Other mammalian ADP-ribosyl transferases only attach a single ADP-ribose moiety onto acceptor molecules and therefore act as mono-ADP-ribosyl transferases (Bock and Chang, 2016). ADP-ribosyl transferases use NAD^+ as a co-substrate to transfer the ADP-ribose moiety from NAD^+ onto an amino acid side chain. Similar to protein kinases, several ADP-ribosyl transferases not only ADP-ribosylate other proteins but also undergo auto-modification (Adamietz, 1987; Muthurajan et al., 2014; Vyas et al., 2014).

Protein ADP-ribosylation remains a poorly characterized PTM in plants. Although enzymes of the ADP-ribosyl transferase family are conserved in all land plants (Lamb et al., 2012; Vainonen et al., 2016), only few ADP-ribosylated acceptor proteins have been characterized (Feng et al., 2015, 2016). In addition, the consequences of protein ADP-ribosylation in plants remain largely unknown. Notably, the best-characterized examples of plant protein modification by ADP-ribosylation come from studies of plant pathogens that transfer effector proteins with ADP-ribosyl transferase activity into plant cells to suppress activation of plant innate immunity (Singer et al., 2004; Fu et al., 2007; Wang et al., 2010; Jeong et al., 2011; Nicaise et al., 2013).

The *Arabidopsis thaliana* genome encodes three PARP proteins (annotated as PARP1-3) with 27–47% sequence identity to *Hs*PARP-1 and *Hs*PARP-2. *Arabidopsis* PARP1 and PARP2 are active enzymes while direct evidence for PARP3 ADP-ribosyl transferase activity is lacking (Babiychuk et al., 1998; Feng et al., 2015). Treatment of *Arabidopsis* with γ-radiation or genotoxic agents activates PARP1 and PARP2 (Song et al., 2015). Based on the analysis of *parp* single and double mutants, PARP1 and PARP2 fulfill partially redundant functions in response to genotoxic stress. Upon treatment of *Arabidopsis* seedlings with the DNA double strand break-inducing agent Bleomycin, PARP2 mediates the majority of detectable poly-ADP-ribosylation (Song et al., 2015). However, based on quantification of DNA damage via the Comet assay, *parp1* mutants show higher levels of DNA damage compared to *parp2* mutants following exposure to methyl methane sulfonate as well as in untreated seedlings (Jia et al., 2013). How DNA damage enhances the enzymatic activity of plant PARPs has not been reported in detail. However, based on sequence conservation between plant PARPs and mammalian homologs, the access of NAD^+ to the active site might be blocked by a protein regulatory domain (PRD) located N-terminal to the catalytic domain. Based on the analysis of human PARP-1, sensing of DNA double strand breaks by the N-terminal domains might result in a conformational change of the PRD thereby relieving auto-inhibition of the catalytic domain (Langelier et al., 2012, 2018). In human PARP-1, the binding site for DNA double

strand breaks is formed by two Zinc finger domains and a WGR domain (conserved Trp, Gly, and Arg residues) (Langelier et al., 2012). Similar to human PARP-1, predicted Zinc finger and WGR domains appear to be conserved in *Arabidopsis* PARP1. In contrast, for *Arabidopsis* PARP2, two N-terminal SAP (SAF-A/B, Acinus, and PIAS) domains followed by a WGR domain have been predicted suggesting that the mechanism of PARP2 activation by DNA damage differs from PARP1 (Lamb et al., 2012; Vainonen et al., 2016).

PARP1 and PARP2 localize to the plant cell nucleus consistent with their roles in DNA damage repair (Babiychuk et al., 2001; Song et al., 2015). Given their entirely nuclear localization and predicted molecular weights of 111 (PARP1) and 72 (PARP2) kDa, an active nuclear import mechanism for plant PARPs is likely. For PARP2 Babiychuk et al. (2001) reported that a GFP fusion of an N-terminal fragment spanning amino acids 1–104 is entirely nuclear localized, indicating an active import mechanism. Active transport processes through nuclear pore complexes are mediated by several distinct transport systems. Karyopherins of the importin-α/β group function as adapter proteins that bind cargoes with exposed nuclear localization sequences (NLS) in the cytoplasm, transport them through nuclear pore complexes and release their cargoes in the nucleoplasm (Christie et al., 2016). While importin-β proteins can achieve active transport across the nuclear envelope by directly interacting with Phe/Gly-rich repeats of nucleoporins that line the nuclear pore channel (Allen et al., 2001; Bayliss et al., 2002), importin-α proteins form a ternary complex with their cargoes and importin-β for transport to the nucleus (Weis et al., 1996; Cingolani et al., 1999). In *Arabidopsis*, there are nine importin-α isoforms that show both redundant but also specific transport functions (Huang et al., 2010; Merkle, 2011; Wirthmueller et al., 2013; Roth et al., 2017). While the NLS that mediate binding to importin-β can diverge in sequence (Christie et al., 2016), importin-α proteins bind canonical mono- and bipartite NLS characterized by Lys/Arg-rich consensus sequences (Kosugi et al., 2009a; Marfori et al., 2011, 2012). Here we identify an NLS in PARP2 that is sufficient and required for nuclear import. We further demonstrate that this NLS mediates binding to *Arabidopsis* lMPORTIN-α2 in plant cell extracts.

MATERIALS AND METHODS

Plants and Growth Conditions

Nicotiana benthamiana plants were grown in a green house at 22°C/20°C day/night temperatures and 16 h (06:00 to 22:00) supplemental light (200–230 μmol m^2 s^{-1}) from tungsten lamps.

Generation of Plant and *Escherichia coli* Expression Constructs

The following Gateway-compatible pENTR4 plasmids were generated for this work: pENTR4-PARP2, pENTR4-PARP2$^{SAP-WGR}$, pENTR4-PARP2$^{PRD-CAT}$, pENTR4-PARP2^{SAP}, pENTR4-PARP2^{WGR}, pENTR4-PARP2$^{48-51AAAA}$, pENTR4-PARP2$^{48-51QMQL}$, pENTR4-PARP2$^{SAP48-51AAAA}$, pENTR4-PARP2$^{SAP48-51QMQL}$, and pENTR4-PARP2$^{SAP92/93AA}$.

All pENTR4 constructs lack a stop codon for translational fusion to xFP reporters. PARP2 mutant constructs were generated either by the QuikChange method (pENTR4-PARP2$^{48-51AAAA}$ and pENTR4-PARP2$^{SAP92/93AA}$) or by splice-by-overlap-extension (SOE) PCR (pENTR4-PARP2$^{48-51QMQL}$). To generate translational fusions between PARP2 variants and xFP tags, Gateway LR reactions between PARP2 (or PARP2 deletion) constructs and pK7FWG2 (enhanced GFP tag), or pH7RWG2 (RFP tag) (Karimi et al., 2002) were performed. The IMPORTIN-α6:GFP construct was created by an LR reaction between pENTR/D-Topo IMPORTIN-α6 (Roth et al., 2017) and pK7FWG2. The other GFP-tagged importin-α plant expression constructs and the RFP/YFP-tagged HaRxL106 constructs have been described previously (Wirthmueller et al., 2015).

To generate the *E. coli* expression construct for ΔIBB IMPORTIN-α2 [lacking the auto-inhibitory importin-β-binding (IBB) domain], a cDNA fragment coding for amino acids 75–535 was amplified and cloned into KpnI/HindIII-linearized pOPINF (Berrow et al., 2007) via Gibson assembly. The *E. coli* PARP2 SAP (amino acids 1–105) expression construct was generated following the same strategy but using pOPINS3C (Bird, 2011) as expression plasmid. For production of α-GFP affinity beads, the coding sequence of an α-GFP nanobody (Addgene plasmid #49172; Kubala et al., 2010) was fused in frame with a Gly-Gly-Ser-Gly-Ser linker and the Halo tag from plasmid pGW-nHalo (Peterson and Kwon, 2012) into pOPINE (Berrow et al., 2007) via Gibson assembly. See **Supplementary Table S1** for oligo nucleotides and cloning methods.

Transient Protein Expression in *N. benthamiana*

For transient expression in *N. benthamiana* leaves binary vectors were transformed into *Agrobacterium tumefaciens* strain GV3101::pMP90 (or GV3101::pMP90RK for YFP:HaRxL106). Agrobacteria were plated on YEB medium with appropriate antibiotics and incubated for 3 days at 28°C. On the day of infiltration, the cells were resuspended in infiltration medium (10 mM MES pH 5.6, 10 mM MgCl$_2$) and the OD$_{600}$ was adjusted to 0.8. To suppress transgene silencing Agrobacteria expressing the tomato bushy stunt virus 19K silencing suppressor were co-infiltrated. The culture of the 19K strain was adjusted to an OD$_{600}$ of 6.0. After adding Acetosyringone to a final concentration of 100 μM the bacteria were incubated for 2 h at RT and then mixed in a ratio of xFP[20]:19K[3] for localization experiments or G/YFP[10]:RFP[10]:19K[3] for co-immunoprecipitation and co-localization experiments. *Agrobacterium* mixtures were infiltrated with a needleless syringe into leaves of 4–5 week-old *N. benthamiana* plants and leaf material was harvested for microscopy or protein extraction 72 h later.

Confocal Microscopy

Leaf discs excised from *N. benthamiana* were mounted on microscope slides in water and the subcellular localization of xFP-tagged proteins was analyzed using a Leica TCS SP5 confocal unit attached to a Leica DMI6000 CS microscope. GFP and YFP were excited at 488 nm and collected at 500–525 nm and 525–540 nm,

respectively. RFP was excited at 561 nm and collected at 580–610 nm. The gain setting of the confocal unit was adjusted to just below the threshold for saturation of the signal. Images were acquired and analyzed using LAS AF software (Leica).

Plant Protein Extraction, Immunoprecipitation and Detection

Protein extracts were prepared by grinding *N. benthamiana* leaf material in liquid nitrogen to a fine powder followed by resuspension in extraction buffer [50 mM Tris, 150 mM NaCl, 10% Glycerol, 1 mM EDTA, 5 mM DTT, 1x Plant Protease Inhibitor Cocktail (Sigma P9599)[1], pH 7.5] at a ratio of 2 ml buffer per 1 g leaf material. The extracts were centrifuged at 20000 x *g*/4°C/20 min and the supernatant was either boiled in Sodium dodecyl sulfate (SDS) sample buffer for western blots or used for co-immunoprecipitation experiments. For western blots protein samples were separated by SDS-PAGE and electro-blotted onto nitrocellulose membrane. Antibodies used were α-GFP 210-PS-1GP (Amsbio)[2] and α-mCherry ab125096 (Abcam)[3]. For co-immunoprecipitation a fraction of the supernatant was saved as 'input' sample and 15 μl of α-GFP-nanobody:Halo:His6 magnetic beads (see below) were added to 1.4 ml of the remaining supernatant. The samples were incubated on a rotating wheel at 4°C for 2 h followed by collection of the beads using a magnetic sample tube rack. The beads were washed 3 times with 1 ml extraction buffer and then boiled in 40 μl SDS sample buffer to elute protein from the beads.

Protein Expression and Purification

For protein expression in *E. coli,* pOPINS3C carrying His6:SUMO:SAP and pOPINE carrying the α-GFP-nanobody:Halo:His6 construct (Addgene plasmid #111090) were transformed into SHuffle® T7 Competent *E. coli* cells (New England Biolabs). The His6:ΔIBB-IMPORTIN-α2 protein was expressed from pOPINF in SoluBL21 cells (Genlantis). All cultures were grown to an OD$_{600}$ of 1 to 1.2 at 37°C, then shifted to 18°C and expression was induced by addition of 0.5 mM IPTG. After 16-18 h the bacteria were harvested by centrifugation (5000 × *g*, 12 min.). His6-tagged proteins were purified using a combination of immobilized metal ion affinity chromatography and size exclusion chromatography. To this end, the cell pellets were resuspended in 50 mM Tris, 300 mM NaCl, 50 mM Glycine, 20 mM Imidazole, 5% Glycerol, pH 8.0 at a ratio of 20 ml per initial liter of culture volume. Bacterial lysis was achieved by incubation with Lysozyme (20 min., RT) followed by sonication (2 times 2 min. at level 4 on a Branson Sonifier 150). The cell extract was cleared from debris and insoluble proteins by centrifugation (30000 × *g*, 4°C, 20 min) and the supernatant was loaded onto pre-equilibrated Ni^{2+}-immobilized metal ion affinity chromatography columns (His-Trap HP 5 ml, GE Healthcare). After washing out unbound proteins, His6-tagged proteins were eluted with 50 mM Tris, 300 mM NaCl, 50 mM Glycine, 250 mM Imidazole, 5% Glycerol,

[1] http://www.sigmaaldrich.com

[2] http://www.amsbio.com

[3] http://www.abcam.com

pH 8.0 and directly injected onto Hi-Load 26/60 Superdex 75 (His6:SUMO:SAP, α-GFP-nanobody:Halo:His6) or Superdex 200 (His6:ΔIBB-IMPORTIN-α2) size exclusion columns (GE Healthcare) using buffer A4 (20 mM HEPES, 150 mM NaCl, pH 7.5) as the elution buffer. Proteins were concentrated using ultrafiltration columns (Sartorius), frozen in liquid nitrogen and stored at −80°C.

Analytical Size Exclusion Chromatography

Purified His6:ΔIBB-IMPORTIN-α2 or His6:SUMO:SAP was injected onto a Superdex 200 10/300 GL size exclusion column (GE Healthcare) in a volume of 1 ml. Proteins were eluted from the column with buffer A4 at a flow rate of 0.4 ml/min and 1 ml fractions were collected. These fractions were subsequently analyzed by SDS-PAGE and Instant Blue (Expedeon) staining.

Production of GFP Affinity Magnetic Beads

To couple the α-GFP nanobody:Halo:His6 fusion protein to magnetic beads, 250 ml of Magne® HaloTag® Beads (Promega) were washed in 1 ml A4 buffer and the beads were collected using a magnetic sample tube rack. 1.5 mg of the α-GFP nanobody:Halo:His6 protein was mixed with the washed beads in 2 ml buffer A4 and incubated on a rotating wheel for 2 h at 4°C and 15 rpm. The magnetic beads were collected and washed three times with 1 ml A4 buffer. The affinity beads were stored in 250 μl of storage buffer (50 mM HEPES, 150 mM NaCl, 15% Glycerol, 0.05% NaN$_3$, pH 7.5) at 4°C until use.

Accession Numbers

A. thaliana PARP2 (AT4G02390), IMPORTIN-α1 (AT3G06720), IMPORTIN-α2 (AT4G16143), IMPORTIN-α3/MOS6 (AT4G02150), IMPORTIN-α4 (AT1G09270), IMPORTIN-α6 (AT1G02690), IMPORTIN-α9 (AT5G03070); *Hyaloperonospora arabidopsidis* effector protein HaRxL106 (GenBank HE574762.1).

RESULTS

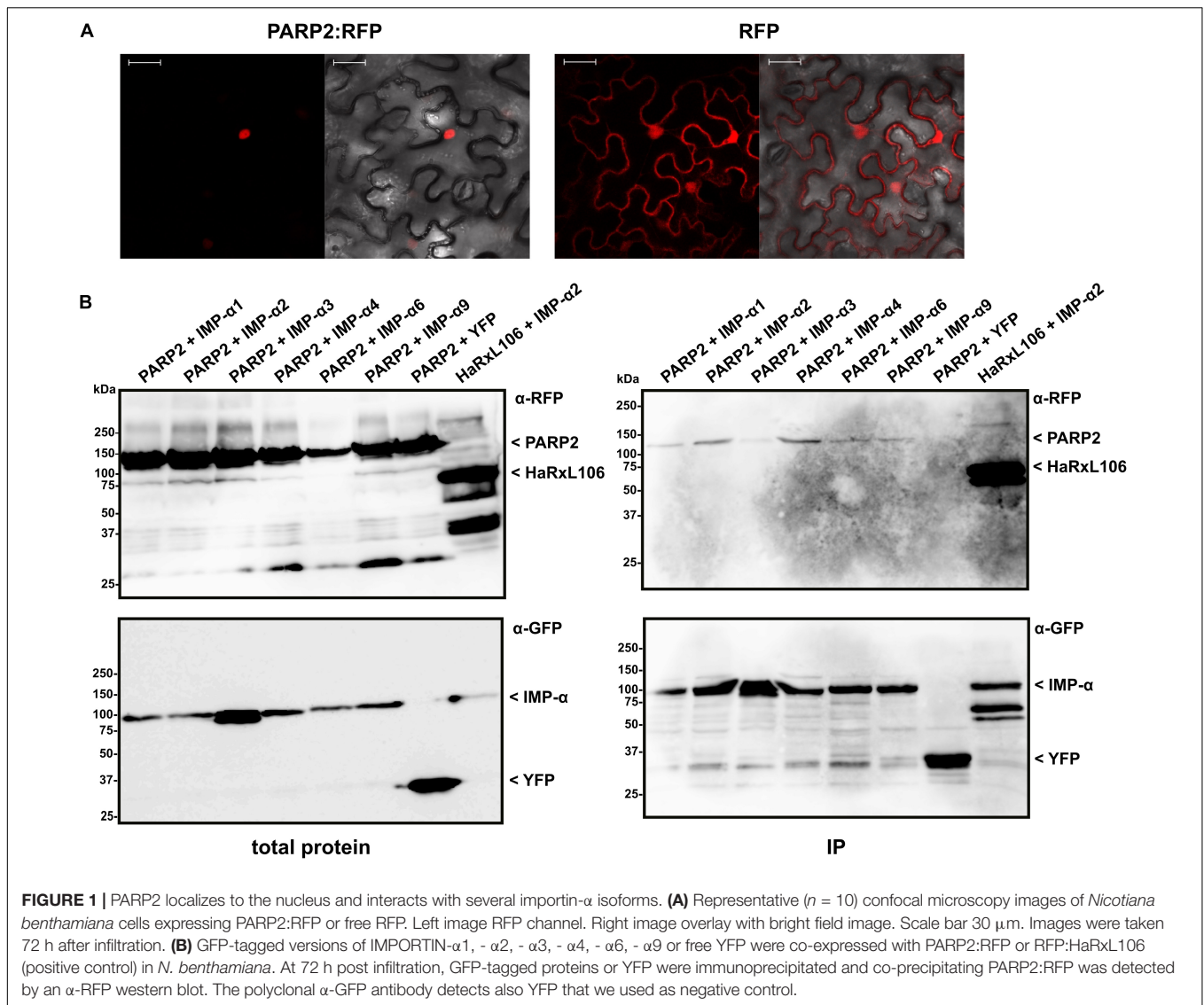## PARP2 Interacts With Several Importin-α Proteins

We expressed PARP2:RFP in epidermal cells of *N. benthamiana* and confirmed that the fusion protein localized to the nucleus (**Figure 1A**). PARP2:RFP co-localized with a YFP-tagged form of the oomycete effector protein HaRxL106 that we used as a nuclear marker as it is actively transported into nuclei when expressed in plant cells (**Supplementary Figure S1**; Wirthmueller et al., 2015). In contrast, free RFP showed a nucleo-cytoplasmic distribution, which is in accordance with unrestricted passive diffusion of macromolecules of molecular weights below 40–60 kDa through nuclear pore complexes (**Figure 1**; Timney et al., 2016). To test for interaction with importin-α, we co-expressed PARP2:RFP with the six importin-α proteins

that are expressed in *Arabidopsis* leaf tissue (IMPORTIN-α1-4, IMPORTIN-α6, IMPORTIN-α9; Wirthmueller et al., 2013). For immunoprecipitation, and based on the finding that a C-terminal GFP tag does not interfere with IMPORTIN-α3 function (Palma et al., 2005), we expressed all importin-α proteins as N-terminal fusions to GFP. When expressed in *N. benthamiana*, IMPORTIN-α:GFP fusions showed a predominantly nuclear localization as previously reported (see **Supplementary Figure S1** for IMPORTIN-α2:GFP as example; Kanneganti et al., 2007). As shown in **Figure 1B**, PARP2:RFP co-precipitated with several importin-α isoforms. In three independent experiments we observed a trend for stronger interaction between PARP2 and IMPORTIN-α2 and IMPORTIN-α4 compared to the other importin-α proteins (**Figure 1B** and **Supplementary Figure S2**). PARP2:RFP showed no interaction with YFP that we used as negative control (**Figure 1B** and **Supplementary Figure S2**). Compared to the previously characterized interaction between IMPORTIN-α2 and the oomycete effector protein HaRxL106 that binds to importin-α with a dissociation constant in the low micro-molar range (Wirthmueller et al., 2015), PARP2:RFP showed relatively weak binding to importin-α proteins (**Figure 1B** and **Supplementary Figure S2**).

A Nuclear Localization Sequence Located Between the PARP2 SAP Domains Is Sufficient and Required for Nuclear Import

To map sequences of PARP2 that are required for nuclear import we generated truncated variants of the protein and expressed these as GFP fusions in *N. benthamiana*. Based on the predicted domain structure of PARP2 (**Figure 2A**), we initially split the protein between the WGR domain and the protein regulatory domain (PRD). The fusion of the SAP-WGR domains to GFP retained an entirely nuclear localization (**Figure 2B**). In contrast, a GFP fusion of the PARP2 fragment comprising PRD and catalytic (CAT) domains showed a nucleo-cytoplasmic distribution (**Figure 2B**). Therefore, the sequence(s) for active nuclear import of PARP2 are located within the first 280 amino acids of the protein and the regulatory and catalytic domains do not contain additional NLS. We then expressed the isolated SAP and WGR domains as GFP fusions in *N. benthamiana*. The SAP:GFP fusion showed an entirely nuclear localization while the WGR:GFP signal was distributed between the cytoplasm and the nucleus (**Figure 2B**). This suggests that all nuclear targeting sequences of PARP2 are located within the first 127 amino acids of the protein that are predicted to fold into two SAP domains (Lamb et al., 2012; Vainonen et al., 2016).
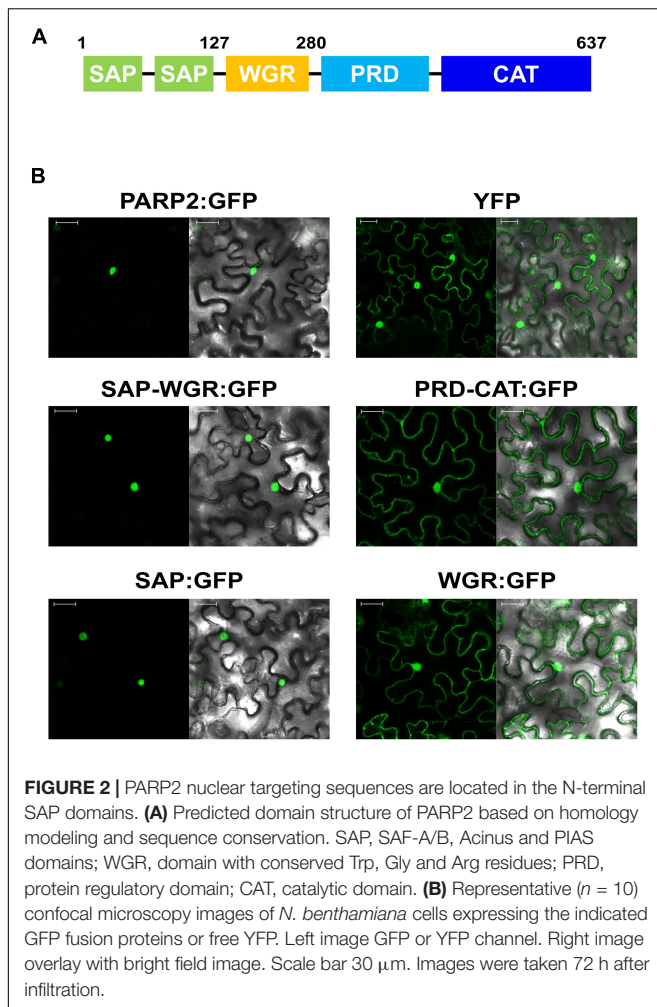
Having mapped the NLS of PARP2 to the N-terminal 127 amino acids, we focused on clusters of basic amino acids that could constitute an NLS. Using NLS Mapper (Kosugi et al., 2009b), we identified a candidate monopartite NLS (SKSKRKRNS; amino acids 45–53; NLS Mapper score 7.0) that might be part of a larger bipartite NLS (KSKRKRNSSNDTYESNKLIAI, amino acids 46–66; NLS

FIGURE 1 | PARP2 localizes to the nucleus and interacts with several importin-α isoforms. **(A)** Representative (*n* = 10) confocal microscopy images of *Nicotiana benthamiana* cells expressing PARP2:RFP or free RFP. Left image RFP channel. Right image overlay with bright field image. Scale bar 30 μm. Images were taken 72 h after infiltration. **(B)** GFP-tagged versions of IMPORTIN-α1, - α2, - α3, - α4, - α6, - α9 or free YFP were co-expressed with PARP2:RFP or RFP:HaRxL106 (positive control) in *N. benthamiana*. At 72 h post infiltration, GFP-tagged proteins or YFP were immunoprecipitated and co-precipitating PARP2:RFP was detected by an α-RFP western blot. The polyclonal α-GFP antibody detects also YFP that we used as negative control.

Mapper score 6.5). We mutated the KRKR motif of the candidate NLS either to a quadruple Alanine or the sequence QMQL. The latter sequence is more similar to KRKR with respect to the length of amino acid side chains but does not carry a positive charge. When we transiently expressed the corresponding mutant SAP:RFP fusions in *N. benthamiana* we observed a nucleo-cytoplasmic distribution of the RFP signal, indicating that PARP2 amino acids 48–51 are indeed part of an NLS (**Figure 3A**). In contrast, changing two other basic amino acids of PARP2 (K92/K93) to Alanine did not result in a nucleo-cytoplasmic distribution (**Figure 3A**). We then introduced the AAAA and QMQL NLS mutations into full-length PARP2 and analyzed the subcellular localization of the respective fusion proteins. As shown in **Figure 3A**, both mutations in the NLS resulted in a predominantly cytoplasmic localization of PARP2:RFP with strong depletion of the signal from the nucleus. In cases where we observed a residual RFP signal from the nucleus the fluorescence was stronger at the nuclear envelope

(**Figure 3B** and **Supplementary Figure S1**). Therefore amino acids 48–51 are essential for nuclear import of PARP2 and, based on the cytoplasmic localization of the NLS mutant variants, it appears unlikely that PARP2 has other strong nuclear targeting sequences.

To test whether nuclear import of PARP2 correlates with binding to importin-α, we performed co-immunoprecipitation experiments between IMPORTIN-α2 and mutated variants of the isolated SAP domains and full-length PARP2. As shown in **Figure 3C**, mutation of the KRKR motif resulted in weaker or non-detectable binding of the SAP domains to IMPORTIN-α2 (see **Supplementary Figure S3** for data from two additional independent experiments). Likewise, PARP2 variants with mutations of the KRKR motif showed quantitatively reduced or no detectable binding to IMPORTIN-α2 (**Figure 3D** and **Supplementary Figure S4**). Overall, we observed a correlation between the strength of IMPORTIN-α2 binding and nuclear localization for the isolated SAP domains and full-length PARP2.

FIGURE 2 | PARP2 nuclear targeting sequences are located in the N-terminal SAP domains. **(A)** Predicted domain structure of PARP2 based on homology modeling and sequence conservation. SAP, SAF-A/B, Acinus and PIAS domains; WGR, domain with conserved Trp, Gly and Arg residues; PRD, protein regulatory domain; CAT, catalytic domain. **(B)** Representative (*n* = 10) confocal microscopy images of *N. benthamiana* cells expressing the indicated GFP fusion proteins or free YFP. Left image GFP or YFP channel. Right image overlay with bright field image. Scale bar 30 µm. Images were taken 72 h after infiltration.

These results are consistent with importin-α-dependent nuclear import of PARP2 mediated by the NLS comprising the KRKR motif.

The PARP2 SAP Domains and IMPORTIN-α2 Do Not Form a Stable Complex *in vitro*

Several NLS bind to importin-α with affinities in or below the low micro-molar range (Hübner et al., 1999; Hodel et al., 2006; Timney et al., 2006; Kosugi et al., 2008; Chang et al., 2012). This often allows for isolation of a stable protein complex between NLS peptides and the Armadillo repeat domains of importin-α proteins (Conti et al., 1998; Fontes et al., 2003; Marfori et al., 2012). In comparison to the interaction between the oomycete effector HaRxL106 and IMPORTIN-α3, for which a stable complex could be detected (Wirthmueller et al., 2015), PARP2 showed weaker binding to all tested importin-α isoforms (**Figure 1B**). To test for protein complex formation between the SAP domains of PARP2 and IMPORTIN-α2, we expressed the SAP domains (amino acids 1–105) and the Armadillo repeat domain of IMPORTIN-α2 (amino acids 75–535) as His6-tagged proteins in *E. coli* (for the SAP domains we

produced a His6:SUMO:SAP fusion, see methods for details). We purified both proteins by immobilized metal ion affinity and subsequent size exclusion chromatography, mixed the proteins in a 1:2 (IMPORTIN-α2:SAP) molar ratio and assessed complex formation by analytical size exclusion chromatography. As shown in **Figure 4A**, the IMPORTIN-α2 and SAP proteins eluted in separate peaks when injected individually onto the size exclusion column. When we mixed the two proteins we did not detect a higher molecular weight peak. Analyzing the eluted fraction by SDS-PAGE showed that the elution profile of IMPORTIN-α2 was not altered by the onefold molar excess of the PARP2 SAP domains (**Figure 4B** and **Supplementary Figure S5**). This suggests that unlike other importin-α/NLS pairs the PARP2 SAP domains do not form a stable complex with IMPORTIN-α2 under the conditions tested here. As we have not been successful in expressing the SAP domains with a shorter affinity tag, we could not assess whether the His6:SUMO tag N-terminal to the PARP2 SAP domains might interfere with IMPORTIN-α2 binding.

DISCUSSION

We present evidence for an active importin-α-mediated nuclear import of *Arabidopsis* PARP2. This model is supported by (i) the identification of an NLS in PARP2 that is sufficient and required for nuclear import and (ii) binding studies showing that this NLS mediates interaction with IMPORTIN-α2 in plant cells (**Figures 2**, **3**). PARP2 preferentially bound to IMPORTIN-α2 and IMPORTIN-α4 although we detected weaker interactions with other importin-α isoforms (**Figure 1B** and **Supplementary Figure S2**). This is consistent with partially redundant functions of importin-α isoforms in nuclear transport although examples of specific importin-α/cargo interactions have also been reported (Palma et al., 2005; Timney et al., 2006; Bhattacharjee et al., 2008; Wirthmueller et al., 2015; Roth et al., 2017).

While in some experiments mutation of the KRKR motif in PARP2 completely abolished binding to IMPORTIN-α2, we observed a quantitative reduction of the interaction in other experiments (**Figures 3C,D** and **Supplementary Figures S3, S4**). Based on the NLS Mapper prediction it is possible that the KRKR motif is part of a larger bipartite NLS. Two clusters of basic amino acids that make contact to the major and minor NLS binding sites of importin-α, respectively, characterize canonical bipartite NLS (Marfori et al., 2011). Therefore, the weak association between NLS mutant variants of the SAP domains or full-length PARP2 and IMPORTIN-α2 that we observed in some experiments could be due to other basic amino acids that contribute to importin-α binding. However, the cytoplasmic localization of PARP2 NLS mutant variants (**Figure 3A**) suggests that if such a second contact point between PARP2 and importin-α exists it is not sufficient for nuclear import.

The NLS that we identified here is located between the two predicted SAP domains of PARP2. The location of the NLS in a short stretch of amino acids with no predicted secondary structure is consistent with the finding that NLS are
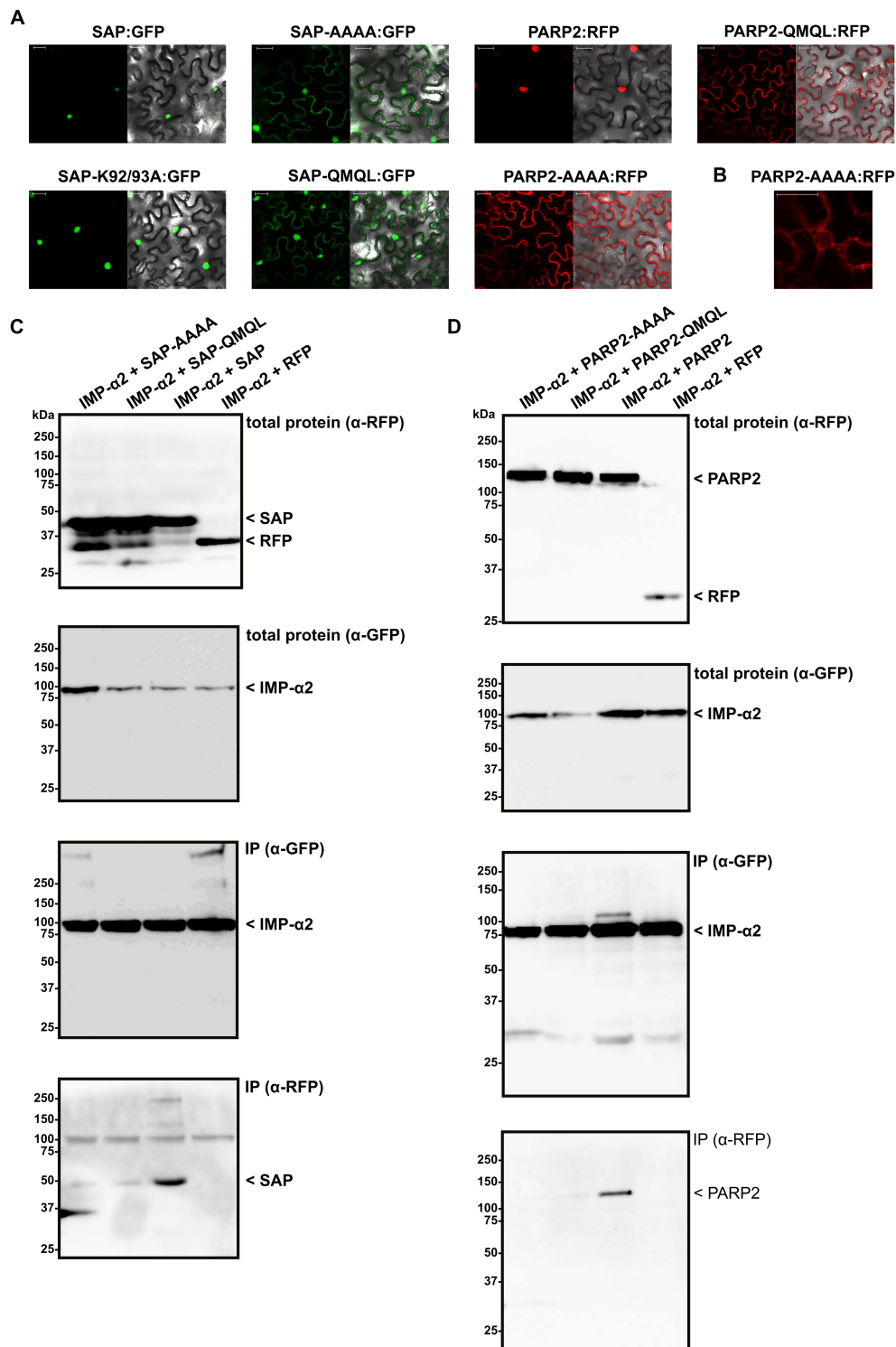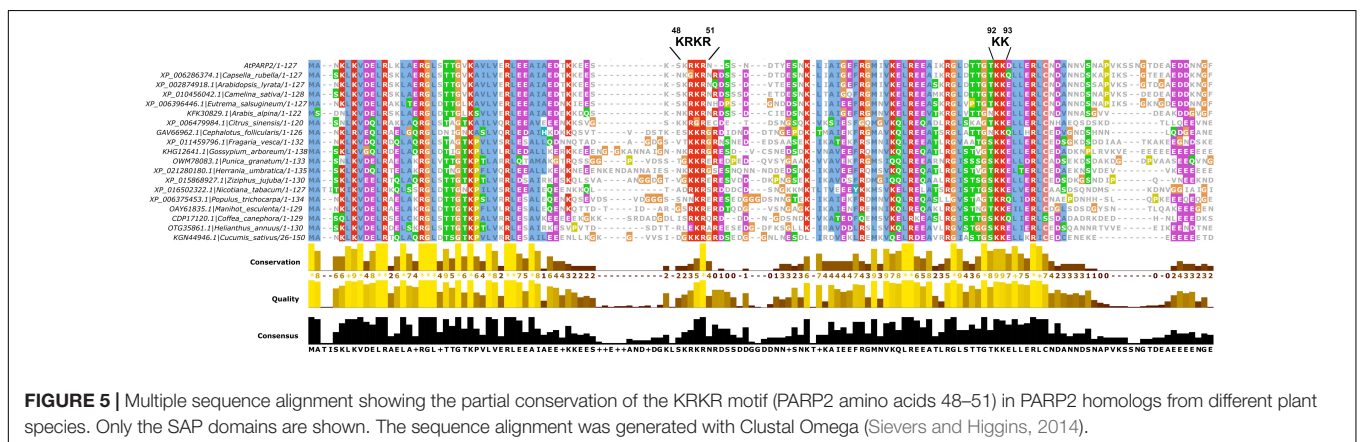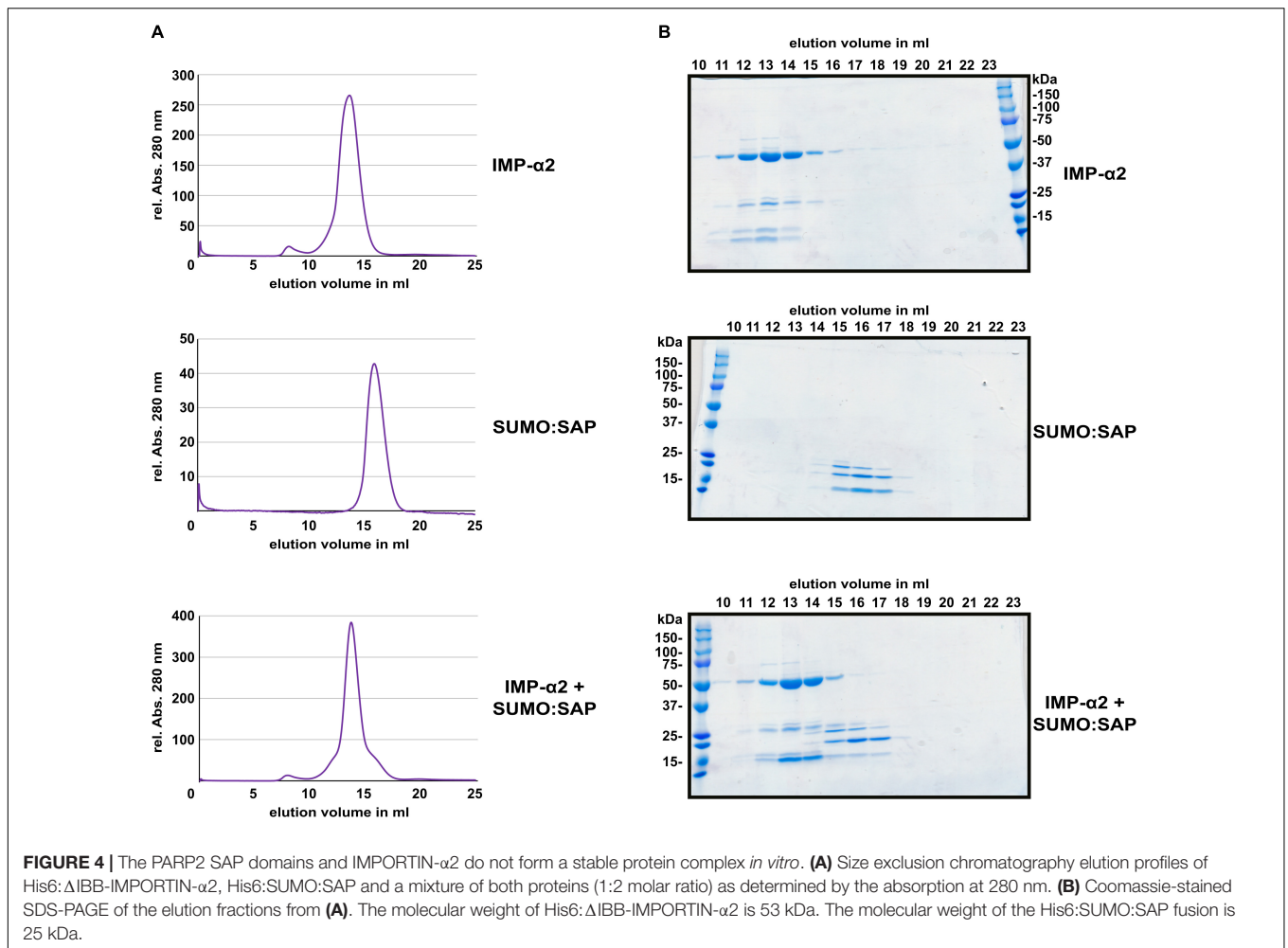
FIGURE 3 | PARP2 amino acids 48–51 are essential for nuclear targeting and mediate interaction with IMPORTIN-α2. **(A)** Representative (*n* = 10) confocal microscopy images of *N. benthamiana* cells expressing the indicated GFP/RFP fusion proteins. Left image GFP or RFP channel. Right image overlay with bright field image. Scale bar 30 μm. Images were taken 72 h after infiltration. 'AAAA' indicates mutation of PARP2 amino acids 48–51 to quadruple Ala. 'QMQL' indicates mutation of PARP2 amino acids 48–51 to Gln-Met-Gln-Leu. 'K92/93A' indicates mutation of PARP2 Lys 92 and 93 to Ala. **(B)** Distribution of the RFP signal from PARP2-AAAA:RFP around a nucleus (*n* = 4). **(C)** IMPORTIN-α2:GFP was co-expressed with free RFP or the indicated RFP-tagged variants of the PARP2 SAP domains in *N. benthamiana*. At 72 h post infiltration, IMPORTIN-α2:GFP was immunoprecipitated and co-precipitating RFP-tagged proteins were detected by an α-RFP western blot. **(D)** Co-immunoprecipitation experiment as in **(C)** but with the wildtype and mutated full-length PARP2 sequences instead of the SAP domains.

FIGURE 4 | The PARP2 SAP domains and IMPORTIN-α2 do not form a stable protein complex *in vitro*. **(A)** Size exclusion chromatography elution profiles of His6:ΔIBB-IMPORTIN-α2, His6:SUMO:SAP and a mixture of both proteins (1:2 molar ratio) as determined by the absorption at 280 nm. **(B)** Coomassie-stained SDS-PAGE of the elution fractions from **(A)**. The molecular weight of His6:ΔIBB-IMPORTIN-α2 is 53 kDa. The molecular weight of the His6:SUMO:SAP fusion is 25 kDa.

FIGURE 5 | Multiple sequence alignment showing the partial conservation of the KRKR motif (PARP2 amino acids 48–51) in PARP2 homologs from different plant species. Only the SAP domains are shown. The sequence alignment was generated with Clustal Omega (Sievers and Higgins, 2014).

often located in disordered regions of proteins. The identified NLS at position 48–51 of PARP2 is consistent with data from Babiychuk et al. (2001) who reported that the first 104 amino acids of the protein are sufficient for nuclear import. Based on an alignment of PARP2 sequences from other plant species (**Figure 5**), the KRKR motif is partially conserved in PARP2 homologs. In several of the sequences shown in **Figure 5**,

amino acids with polar side chains or Gly are present at the position corresponding to *Arabidopsis* PARP2 K48. However, in all of these cases an Arg is present five amino acids downstream of the polar amino acid/Gly suggesting that in these sequences the cluster of basic amino acids is slightly shifted. Therefore, a cluster of basic amino acids that could mediate binding to importin-α is conserved in PARP2 homologs.

Notably, also the nuclear targeting signal for mouse PARP2 is located in its N-terminal DNA-binding domain and two Lysine residues that are critical for nuclear import are modified by acetylation (Haenni et al., 2008a,b).

We noticed that in direct comparison to the interaction between IMPORTIN-α2 and the oomycete effector protein HaRxL106, PARP2 showed a comparably weak association with IMPORTIN-α2 as well as other importin-α isoforms (**Figure 1B**). This is also consistent with no detectable interaction between the SAP domains and IMPORTIN-α2 by size exclusion chromatography (**Figure 4**). Although the KRKR motif constitutes a *bona fide* mono-partite NLS core motif (corresponding to positions P2-P5 of NLS residues that make direct contact to importin-α), the flanking amino acids P1, P6 and P7 can influence the affinity for the receptor (Conti et al., 1998; Kosugi et al., 2009a; Dinkel et al., 2016). Positions P1 and P6 show a preference for hydrophobic or basic amino acids or Proline, whereas in the identified PARP2 NLS P1 is Ser_{47} and P6 is Asn_{52}. Acidic residues are favored at P7, which corresponds to Ser_{53} in PARP2. Therefore, the divergence of the NLS flanking residues from the consensus sequence provides a possible explanation for the comparably low affinity of the PARP2 NLS to importin-α. We also note that the two Ser residues in the NLS flanking sequence could indicate regulation of nuclear import rates by phosphorylation. Post-translational modification of amino acids within or adjacent to NLS can alter the affinity for importin-α (Moll et al., 1991; Fontes et al., 2003; Harreman et al., 2003; Róna et al., 2013). Regarding the results with recombinantly expressed proteins (**Figure 4**) it is possible that such a PTM is absent in the *E. coli* expression system.

The reported dissociation constants between NLS and importin-α proteins span a surprisingly large range, which might in part be explained by the different methods employed for their analyses (Marfori et al., 2012; Wirthmueller et al., 2015; de Barros et al., 2018). Although we observed a comparably weak interaction between PARP2 and importin-α in plant cell extracts and no binding *in vitro*, the affinity between PARP2 and importin-α is sufficient for nuclear import in plant cells (**Figure 1A**). In nuclear import assays, the affinity of an NLS to importin-α determines the import rate (Hodel et al., 2006; Kosugi et al., 2009a). Therefore, cargo proteins with 'low-affinity' NLS such as PARP2 might have slower import kinetics. Why NLS with a comparably low affinity for importin-αs evolved and what the

consequences for nuclear import rates of the respective cargoes are, remains to be determined.

In summary, our data suggest that *Arabidopsis* PARP2 is actively transported into the nucleus via importin-α-mediated transport. An NLS comprising - but possibly not limited to - amino acids 48–51 contributes to importin-α binding and is essential for PARP2 nuclear import.

AUTHOR CONTRIBUTIONS

LW designed the research and wrote the manuscript. CC, RDM, RL, and LW performed the research. CC, RDM, and LW contributed to data analysis, collection, or interpretation. All authors have approved the submitted version of the manuscript.

FUNDING

ACKNOWLEDGMENTS

SUPPLEMENTARY MATERIAL

The Supplementary Material for this article can be found online at: https://www.frontiersin.org/articles/10.3389/fpls.2018.01581/full#supplementary-material

REFERENCES

Adamietz, P. (1987). Poly(ADP-ribose) synthase is the major endogenous nonhistone acceptor for poly(ADP-ribose) in alkylated rat hepatoma cells. *Eur. J. Biochem.* 169, 365–372. doi: 10.1111/j.1432-1033.1987.tb13621.x

Allen, N. P., Huang, L., Burlingame, A., and Rexach, M. (2001). Proteomic analysis of nucleoporin interacting proteins. *J. Biol. Chem.* 276, 29268–29274. doi: 10.1074/jbc.M102629200

Asensi-Fabado, M.-A., Amtmann, A., and Perrella, G. (2017). Plant responses to abiotic stress: the chromatin context of transcriptional regulation. *Biochim. Biophys. Acta* 1860, 106–122. doi: 10.1016/j.bbagrm.2016.07.015

Babiychuk, E., Cottrill, P. B., Storozhenko, S., Fuangthong, M., Chen, Y., O'Farrell, M. K., et al. (1998). Higher plants possess two structurally different poly(ADP-ribose) polymerases. *Plant J. Cell Mol. Biol.* 15, 635–645. doi: 10.1046/j.1365-313x.1998.00240.x

Babiychuk, E., Van Montagu, M., and Kushnir, S. (2001). N-terminal domains of plant poly(ADP-ribose) polymerases define their association with mitotic chromosomes. *Plant J. Cell Mol. Biol.* 28, 245–255. doi: 10.1046/j.1365-313X.2001.01143.x

Bai, P. (2015). Biology of Poly(ADP-Ribose) polymerases: the factotums of cell maintenance. *Mol. Cell* 58, 947–958. doi: 10.1016/j.molcel.2015.01.034

Bayliss, R., Littlewood, T., Strawn, L. A., Wente, S. R., and Stewart, M. (2002). GLFG and FxFG nucleoporins bind to overlapping sites on importin-beta. *J. Biol. Chem.* 277, 50597–50606. doi: 10.1074/jbc.M209037200

Berrow, N. S., Alderton, D., Sainsbury, S., Nettleship, J., Assenberg, R., Rahman, N., et al. (2007). A versatile ligation-independent cloning method suitable for high-throughput expression screening applications. *Nucleic Acids Res.* 35:e45. doi: 10.1093/nar/gkm047

Bhattacharjee, S., Lee, L.-Y., Oltmanns, H., Cao, H., Veena, Cuperus, J., et al. (2008). IMPa-4, an *Arabidopsis* importin alpha isoform, is preferentially involved in Agrobacterium-mediated plant transformation. *Plant Cell* 20, 2661–2680. doi: 10.1105/tpc.108.060467

Bird, L. E. (2011). High throughput construction and small scale expression screening of multi-tag vectors in *Escherichia coli. Methods San Diego Calif.* 55, 29–37. doi: 10.1016/j.ymeth.2011.08.002

Bock, F. J., and Chang, P. (2016). New directions in poly(ADP-ribose) polymerase biology. *FEBS J.* 283, 4017–4031. doi: 10.1111/febs.13737

Bock, F. J., Todorova, T. T., and Chang, P. (2015). RNA regulation by Poly(ADP-Ribose) polymerases. *Mol. Cell* 58, 959–969. doi: 10.1016/j.molcel.2015.01.037

Chang, C.-W., Couñago, R. L. M., Williams, S. J., Bodén, M., and Kobe, B. (2012). Crystal structure of rice importin-α and structural basis of its interaction with plant-specific nuclear localization signals. *Plant Cell* 24, 5074–5088. doi: 10. 1105/tpc.112.104422

Christie, M., Chang, C.-W., Róna, G., Smith, K. M., Stewart, A. G., Takeda, A. A. S., et al. (2016). Structural biology and regulation of protein import into the nucleus. *J. Mol. Biol.* 428, 2060–2090. doi: 10.1016/j.jmb.2015.10.023

Cingolani, G., Petosa, C., Weis, K., and Müller, C. W. (1999). Structure of importin-beta bound to the IBB domain of importin-alpha. *Nature* 399, 221–229. doi: 10.1038/20367

Conti, E., Uy, M., Leighton, L., Blobel, G., and Kuriyan, J. (1998). Crystallographic analysis of the recognition of a nuclear localization signal by the nuclear import factor karyopherin alpha. *Cell* 94, 193–204. doi: 10.1016/S0092-8674(00)81419-1

de Barros, A. C., Takeda, A. A. S., Dreyer, T. R., Velazquez-Campoy, A., Kobe, B., and Fontes, M. R. M. (2018). DNA mismatch repair proteins MLH1 and PMS2 can be imported to the nucleus by a classical nuclear import pathway. *Biochimie* 146, 87–96. doi: 10.1016/j.biochi.2017.11.013

Dinkel, H., Van Roey, K., Michael, S., Kumar, M., Uyar, B., Altenberg, B., et al. (2016). ELM 2016–data update and new functionality of the eukaryotic linear motif resource. *Nucleic Acids Res.* 44, D294–D300. doi: 10.1093/nar/gkv1291

Feng, B., Liu, C., de Oliveira, M. V. V., Intorne, A. C., Li, B., Babilonia, K., et al. (2015). Protein poly(ADP-ribosyl)ation regulates *Arabidopsis* immune gene expression and defense responses. *PLoS Genet.* 11:e1004936. doi: 10.1371/journal.pgen.1005294

Feng, B., Ma, S., Chen, S., Zhu, N., Zhang, S., Yu, B., et al. (2016). PARylation of the forkhead-associated domain protein DAWDLE regulates plant immunity. *EMBO Rep.* 17, 1799–1813. doi: 10.15252/embr.201642486

Fontes, M. R. M., Teh, T., Jans, D., Brinkworth, R. I., and Kobe, B. (2003). Structural basis for the specificity of bipartite nuclear localization sequence binding by importin-alpha. *J. Biol. Chem.* 278, 27981–27987. doi: 10.1074/jbc.M303275200

Fu, Z. Q., Guo, M., Jeong, B., Tian, F., Elthon, T. E., Cerny, R. L., et al. (2007). A type III effector ADP-ribosylates RNA-binding proteins and quells plant immunity. *Nature* 447, 284–288. doi: 10.1038/nature05737

Haenni, S. S., Altmeyer, M., Hassa, P. O., Valovka, T., Fey, M., and Hottiger, M. O. (2008a). Importin alpha binding and nuclear localization of PARP-2 is dependent on lysine 36, which is located within a predicted classical NLS. *BMC Cell Biol.* 9:39. doi: 10.1186/1471-2121-9-39

Haenni, S. S., Hassa, P. O., Altmeyer, M., Fey, M., Imhof, R., and Hottiger, M. O. (2008b). Identification of lysines 36 and 37 of PARP-2 as targets for acetylation and auto-ADP-ribosylation. *Int. J. Biochem. Cell Biol.* 40, 2274–2283. doi: 10. 1016/j.biocel.2008.03.008

Harreman, M. T., Cohen, P. E., Hodel, M. R., Truscott, G. J., Corbett, A. H., and Hodel, A. E. (2003). Characterization of the auto-inhibitory sequence within the N-terminal domain of importin alpha. *J. Biol. Chem.* 278, 21361–21369. doi: 10.1074/jbc.M301114200

Hashiguchi, A., and Komatsu, S. (2017). Posttranslational modifications and plant-environment interaction. *Methods Enzymol.* 586, 97–113. doi: 10.1016/bs.mie.2016.09.030

Hodel, A. E., Harreman, M. T., Pulliam, K. F., Harben, M. E., Holmes, J. S., Hodel, M. R., et al. (2006). Nuclear localization signal receptor affinity correlates with in vivo localization in *Saccharomyces cerevisiae. J. Biol. Chem.* 281, 23545–23556. doi: 10.1074/jbc.M601718200

Huang, J.-G., Yang, M., Liu, P., Yang, G.-D., Wu, C.-A., and Zheng, C.-C. (2010). Genome-wide profiling of developmental, hormonal or environmental responsiveness of the nucleocytoplasmic transport receptors in *Arabidopsis. Gene* 451, 38–44. doi: 10.1016/j.gene.2009.11.009

Hübner, S., Smith, H. M., Hu, W., Chan, C. K., Rihs, H. P., Paschal, B. M., et al. (1999). Plant importin alpha binds nuclear localization sequences with high affinity and can mediate nuclear import independent of importin beta. *J. Biol. Chem.* 274, 22610–22617. doi: 10.1074/jbc.274.32.22610

Jeong, B., Lin, Y., Joe, A., Guo, M., Korneli, C., Yang, H., et al. (2011). Structure function analysis of an ADP-ribosyltransferase type III effector and its RNA-binding target in plant immunity. *J. Biol. Chem.* 286, 43272–43281. doi: 10.1074/jbc.M111.290122

Jia, Q., den Dulk-Ras, A., Shen, H., Hooykaas, P. J. J., and de Pater, S. (2013). Poly(ADP-ribose)polymerases are involved in microhomology mediated back-up non-homologous end joining in *Arabidopsis thaliana. Plant Mol. Biol.* 82, 339–351. doi: 10.1007/s11103-013-0065-9

Kanneganti, T.-D., Bai, X., Tsai, C.-W., Win, J., Meulia, T., Goodin, M., et al. (2007). A functional genetic assay for nuclear trafficking in plants. *Plant J. Cell Mol. Biol.* 50, 149–158. doi: 10.1111/j.1365-313X.2007.03029.x

Karimi, M., Inzé, D., and Depicker, A. (2002). GATEWAY vectors for Agrobacterium-mediated plant transformation. *Trends Plant Sci.* 7, 193–195. doi: 10.1016/S1360-1385(02)02251-3

Kleinmanns, J. A., and Schubert, D. (2014). Polycomb and Trithorax group protein-mediated control of stress responses in plants. *Biol. Chem.* 395, 1291–1300. doi: 10.1515/hsz-2014-0197

Kosugi, S., Hasebe, M., Entani, T., Takayama, S., Tomita, M., and Yanagawa, H. (2008). Design of peptide inhibitors for the importin alpha/beta nuclear import pathway by activity-based profiling. *Chem. Biol.* 15, 940–949. doi: 10.1016/j.chembiol.2008.07.019

Kosugi, S., Hasebe, M., Matsumura, N., Takashima, H., Miyamoto-Sato, E., Tomita, M., et al. (2009a). Six classes of nuclear localization signals specific to different binding grooves of importin alpha. *J. Biol. Chem.* 284, 478–485. doi: 10.1074/jbc.M807017200

Kosugi, S., Hasebe, M., Tomita, M., and Yanagawa, H. (2009b). Systematic identification of cell cycle-dependent yeast nucleocytoplasmic shuttling proteins by prediction of composite motifs. *Proc. Natl. Acad. Sci. U.S.A.* 106, 10171–10176. doi: 10.1073/pnas.0900604106

Kubala, M. H., Kovtun, O., Alexandrov, K., and Collins, B. M. (2010). Structural and thermodynamic analysis of the GFP: GFP-nanobody complex. *Protein Sci. Publ. Protein Soc.* 19, 2389–2401. doi: 10.1002/pro.519

Lamb, R. S., Citarelli, M., and Teotia, S. (2012). Functions of the poly(ADP-ribose) polymerase superfamily in plants. *Cell. Mol. Life Sci. CMLS* 69, 175–189. doi: 10.1007/s00018-011-0793-4

Langelier, M.-F., Planck, J. L., Roy, S., and Pascal, J. M. (2012). Structural basis for DNA damage-dependent poly(ADP-ribosyl)ation by human PARP-1. *Science* 336, 728–732. doi: 10.1126/science.1216338

Langelier, M. -F., Zandarashvili, L., Aguiar, P. M., Black, B. E., and Pascal, J. M. (2018). NAD + analog reveals PARP-1 substrate-blocking mechanism and allosteric communication from catalytic center to DNA-binding domains. *Nat. Commun.* 9:844. doi: 10.1038/s41467-018-03234-8

Marfori, M., Lonhienne, T. G., Forwood, J. K., and Kobe, B. (2012). Structural basis of high-affinity nuclear localization signal interactions with importin-α. *Traffic* 13, 532–548. doi: 10.1111/j.1600-0854.2012.01329.x

Marfori, M., Mynott, A., Ellis, J. J., Mehdi, A. M., Saunders, N. F. W., Curmi, P. M., et al. (2011). Molecular basis for specificity of nuclear import and prediction of nuclear localization. *Biochim. Biophys. Acta* 1813, 1562–1577. doi: 10.1016/j.bbamcr.2010.10.013

Merkle, T. (2011). Nucleo-cytoplasmic transport of proteins and RNA in plants. *Plant Cell Rep.* 30, 153–176. doi: 10.1007/s00299-010-0928-3

Moll, T., Tebb, G., Surana, U., Robitsch, H., and Nasmyth, K. (1991). The role of phosphorylation and the CDC28 protein kinase in cell cycle-regulated nuclear import of the *S. cerevisiae* transcription factor SWI5. *Cell* 66, 743–758. doi: 10.1016/0092-8674(91)90118-I

Muthurajan, U. M., Hepler, M. R. D., Hieb, A. R., Clark, N. J., Kramer, M., Yao, T., et al. (2014). Automodification switches PARP-1 function from chromatin architectural protein to histone chaperone. *Proc. Natl. Acad. Sci. U.S.A.* 111, 12752–12757. doi: 10.1073/pnas.1405005111

Nicaise, V., Joe, A., Jeong, B., Korneli, C., Boutrot, F., Westedt, I., et al. (2013). *Pseudomonas* HopU1 modulates plant immune receptor levels by blocking the interaction of their mRNAs with GRP7. *EMBO J.* 32, 701–712. doi: 10.1038/emboj.2013.15

Palma, K., Zhang, Y., and Li, X. (2005). An importin alpha homolog, MOS6, plays an important role in plant innate immunity. *Curr. Biol.* 15, 1129–1135. doi: 10.1016/j.cub.2005.05.022

Peterson, S. N., and Kwon, K. (2012). The HaloTag: improving soluble expression and applications in protein functional analysis. *Curr. Chem. Genomics* 6, 8–17. doi: 10.2174/1875397301206010008

Rissel, D., Heym, P. P., Thor, K., Brandt, W., Wessjohann, L. A., and Peiter, E. (2017). No silver bullet – Canonical Poly(ADP-Ribose) Polymerases (PARPs) are no universal factors of abiotic and biotic stress resistance of *Arabidopsis thaliana*. *Front. Plant Sci.* 8:59. doi: 10.3389/fpls.2017.00059

Róna, G., Marfori, M., Borsos, M., Scheer, I., Takács, E., Tóth, J., et al. (2013). Phosphorylation adjacent to the nuclear localization signal of human dUTPase abolishes nuclear import: structural and mechanistic insights. *Acta Crystallogr. D Biol. Crystallogr.* 69, 2495–2505. doi: 10.1107/S0907444913023354

Roth, C., Lüdke, D., Klenke, M., Quathamer, A., Valerius, O., Braus, G. H., et al. (2017). The truncated NLR protein TIR-NBS13 is a MOS/IMPORTIN-α3 interaction partner required for plant immunity. *Plant J. Cell Mol. Biol.* 92, 808–821. doi: 10.1111/tpj.13717

Sievers, F., and Higgins, D. G. (2014). Clustal omega. *Curr. Protoc. Bioinform.* 48, 3.13.1–3.13.16. doi: 10.1002/0471250953.bi0313s48

Singer, A. U., Desveaux, D., Betts, L., Chang, J. H., Nimchuk, Z., Grant, S. R., et al. (2004). Crystal structures of the type III effector protein AvrPphF and its chaperone reveal residues required for plant pathogenesis. *Struct. Lond. Engl.* 1993, 1669–1681. doi: 10.1016/j.str.2004.06.023

Song, J., Keppler, B. D., Wise, R. R., and Bent, A. F. (2015). PARP2 is the predominant poly(ADP-Ribose) polymerase in *Arabidopsis* DNA damage and immune responses. *PLoS Genet.* 11:e1005200. doi: 10.1371/journal.pgen.1005200

Timney, B. L., Raveh, B., Mironska, R., Trivedi, J. M., Kim, S. J., Russel, D., et al. (2016). Simple rules for passive diffusion through the nuclear pore complex. *J. Cell Biol.* 215, 57–76. doi: 10.1083/jcb.201601004

Timney, B. L., Tetenbaum-Novatt, J., Agate, D. S., Williams, R., Zhang, W., Chait, B. T., et al. (2006). Simple kinetic relationships and nonspecific competition govern nuclear import rates in vivo. *J. Cell Biol.* 175, 579–593. doi: 10.1083/jcb.200608141

Vainonen, J. P., Shapiguzov, A., Vaattovaara, A., and Kangasjärvi, J. (2016). Plant PARPs, PARGs and PARP-like proteins. *Curr. Protein Pept. Sci.* 17, 713–723. doi: 10.2174/1389203717666160419144721

Vyas, S., Matic, I., Uchima, L., Rood, J., Zaja, R., Hay, R. T., et al. (2014). Family-wide analysis of poly(ADP-ribose) polymerase activity. *Nat. Commun.* 5:4426. doi: 10.1038/ncomms5426

Wang, Y., Li, J., Hou, S., Wang, X., Li, Y., Ren, D., et al. (2010). A *Pseudomonas syringae* ADP-ribosyltransferase inhibits *Arabidopsis* mitogen-activated protein kinase kinases. *Plant Cell* 22, 2033–2044. doi: 10.1105/tpc.110.075697

Weis, K., Ryder, U., and Lamond, A. I. (1996). The conserved amino-terminal domain of hSRP1 alpha is essential for nuclear protein import. *EMBO J.* 15, 1818–1825. doi: 10.1002/j.1460-2075.1996.tb00531.x

Wirthmueller, L., Roth, C., Banfield, M. J., and Wiermer, M. (2013). Hop-on hop-off: importin-α-guided tours to the nucleus in innate immune signaling. *Front. Plant Sci.* 4:149. doi: 10.3389/fpls.2013.00149

Wirthmueller, L., Roth, C., Fabro, G., Caillaud, M.-C., Rallapalli, G., Asai, S., et al. (2015). Probing formation of cargo/importin-α transport complexes in plant cells using a pathogen effector. *Plant J. Cell Mol. Biol.* 81, 40–52. doi: 10.1111/tpj.12691

Withers, J., and Dong, X. (2017). Post-translational regulation of plant immunity. *Curr. Opin. Plant Biol.* 38, 124–132. doi: 10.1016/j.pbi.2017.05.004